



МОДИФИЦИРОВАННЫЙ МЕТОД РАЗРЕЗОВ И ЕГО АПРОБАЦИЯ НА ПЛОЩАДКАХ «КАРАДАГ» И «ХУЛУГАЙША»

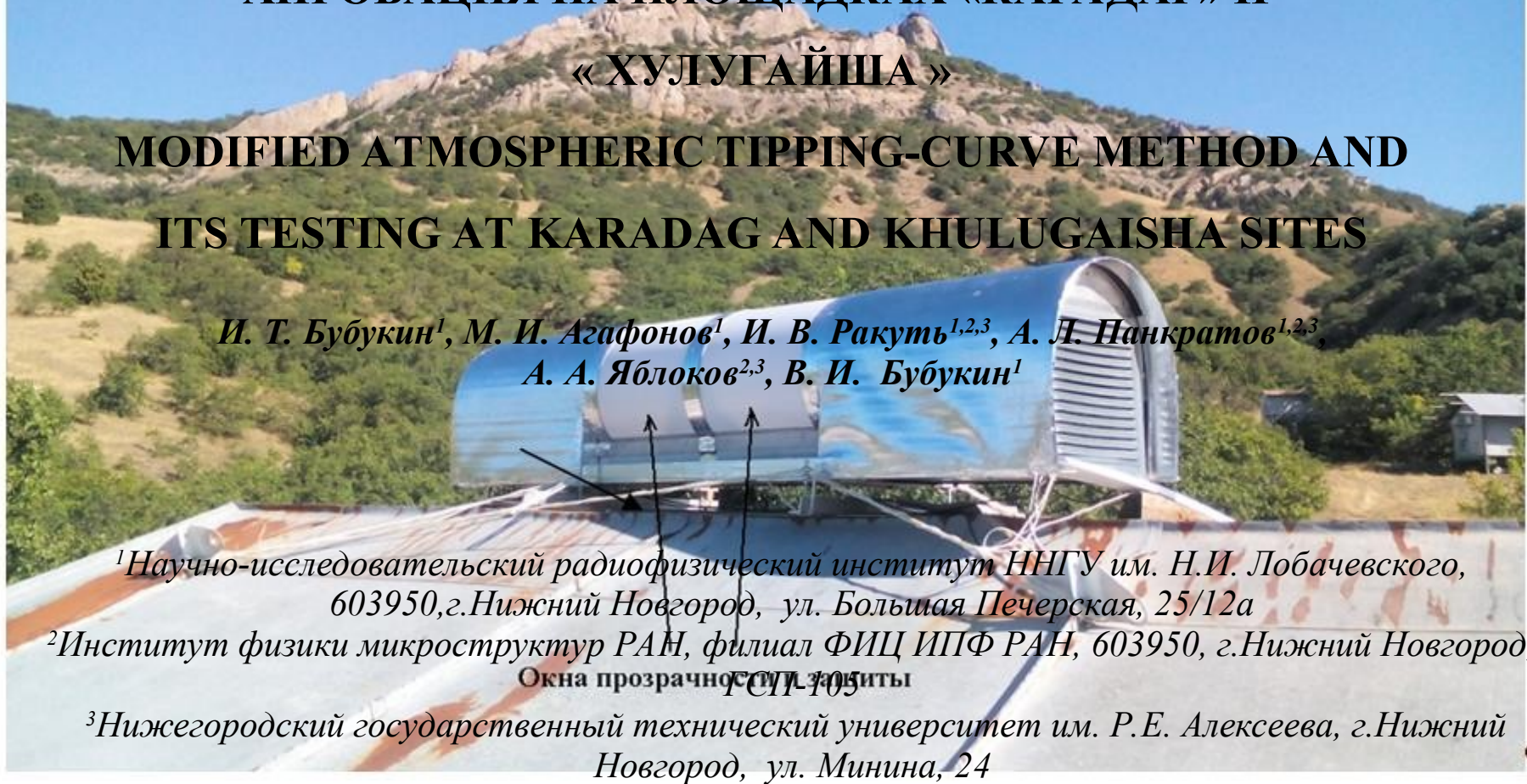
MODIFIED ATMOSPHERIC TIPPING-CURVE METHOD AND ITS TESTING AT KARADAG AND KHULUGAISHA SITES

И. Т. Бубукин¹, М. И. Агафонов¹, И. В. Ракутъ^{1,2,3}, А. Л. Панкратов^{1,2,3},
А. А. Яблоков^{2,3}, В. И. Бубукин¹

¹Научно-исследовательский радиофизический институт ННГУ им. Н.И. Лобачевского,
603950, г.Нижний Новгород, ул. Большая Печерская, 25/12а

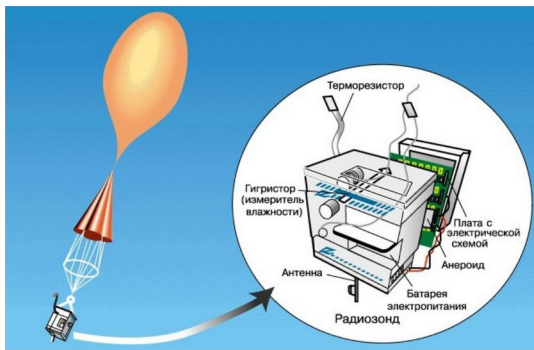
²Институт физики микроструктур РАН, филиал ФИЦ ИПФ РАН, 603950, г.Нижний Новгород,
Окна прозрачности и защиты

³Нижегородский государственный технический университет им. Р.Е. Алексеева, г.Нижний
Новгород, ул. Минина, 24





Most of the weather data is currently obtained using weather stations, which provide only ground-level values of meteorological parameters.



The altitude distributions of meteorological parameters are obtained using balloon probes, which are launched at significant time intervals (2 times a day) and in a limited number of locations.





MTP-5

Meteorological Temperature
profiler (Russia)

[http://www.raimet.ru/equipment/
temperatureprofilers/213/](http://www.raimet.ru/equipment/temperatureprofilers/213/)



Water Vapor Radiometer of the Institute of
Applied Astronomy (IPA) of the Russian
Academy of Sciences (Russia)

<http://iaaras.ru/quasar/wvr/>



Temperature profiler (radiometer)
RPG-HATPRO (Germany)

[http://www.raimet.ru/equipment/
temperatureprofilers/255/#](http://www.raimet.ru/equipment/temperatureprofilers/255/#)



Profiler
TP/WVP-3000 (USA)

Traditionally, atmospheric radiation in the transparency window at a wavelength of 0.8 cm, oxygen and water vapor absorption lines at wavelengths of 0.5 cm and 1.35 cm is used for remote determination of moisture and water reserves, temperature sensing and tropospheric delay of the radio signal.

Frequency Agile Tuning Range	
Water Vapor Band	22-30 GHz
22.235; 23.035; 23.835; 26.235; 30.000	
Oxygen Band	51-59 GHz
51.250; 52.280; 53.850; 54.940; 56.660	
57.290; 58.800	
Minimum Frequency step size	4.0 MHz

Standard channels used for profiles	
MP/WVP-3000	12

Antenna System Optical Resolution	
22-30 GHz	4.9 - 6.3°
51-59 GHz	2.4 - 2.5°

$$\nu_1 \approx 22.235 \text{ GHz}$$

$$\nu_2 \approx 30 \div 40 \text{ GHz}$$

$$\nu_3 \approx 56.7 \text{ GHz}$$

Обычно используется излучение атмосферы в окне прозрачности на длине волны 0.8 см, линиях поглощения кислорода и водяного пара на длинах волн 0.5 см и 1.35 см.

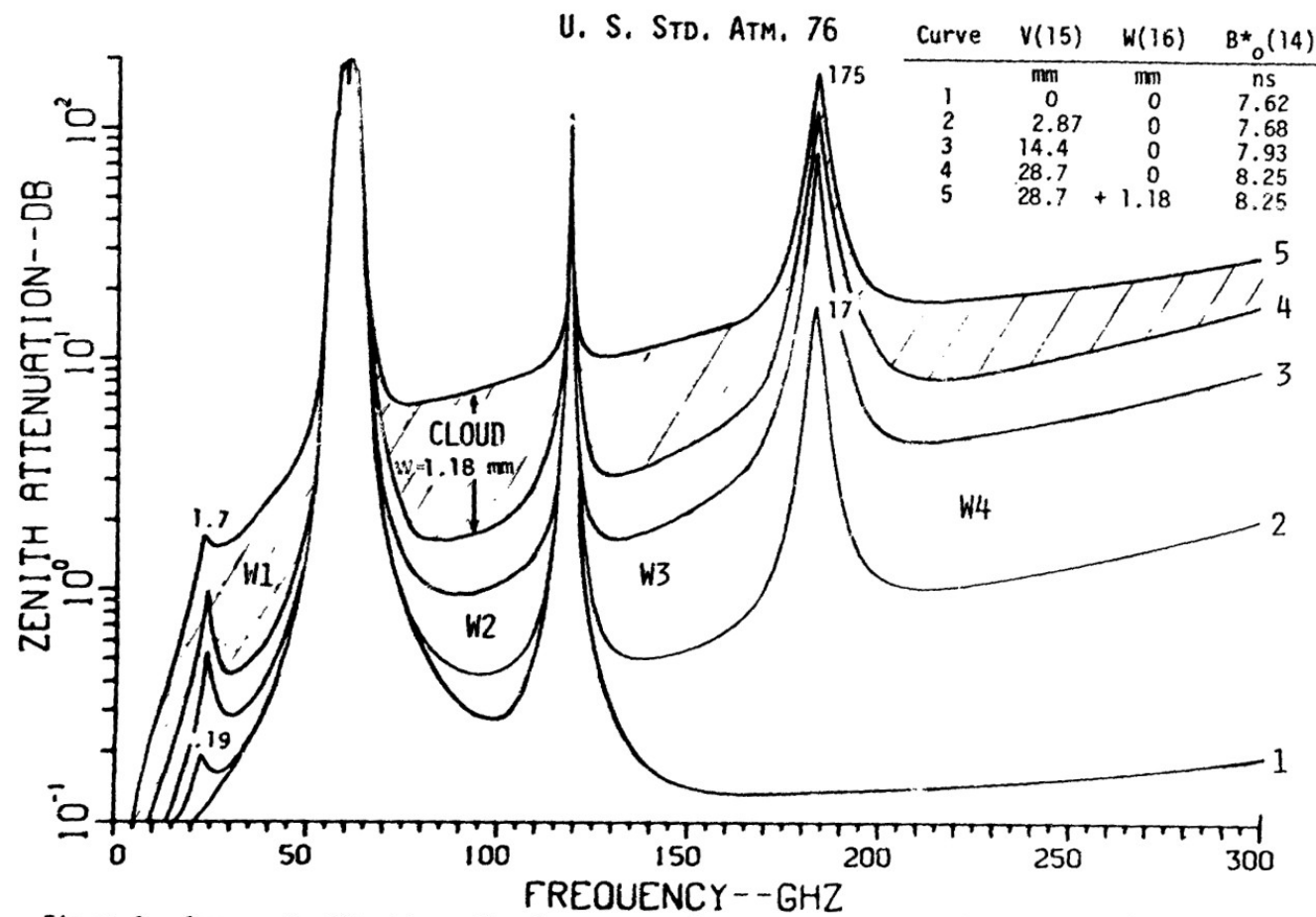


Figure 9. One-way Zenith attenuation A over a frequency range from 5 to 300 GHz (resolution 2.5 GHz) through the U.S. Standard Atmosphere (NOAA, 1976) assuming dry and moist air masses including a rain-bearing cloud calculated with Program P1. The symbols W1 to W4 indicate the millimeter wave window ranges.

Modified atmospheric tipping-curve method for single-wave measurements of atmospheric moisture content and cloud water storage in the millimeter range

$$T_b = \frac{1}{\cos \theta} \int_0^{\infty} T(h) \alpha(h) \exp \left(-\frac{1}{\cos \theta} \int_0^h \alpha(h') dh' \right) dh + T_r \exp \left(-\frac{\tau}{\cos \theta} \right)$$

$$T_b(\theta) = T_{av} \left(1 - e^{-\frac{\tau}{\cos \theta}} \right) + 2.73 \cdot e^{-\frac{\tau}{\cos \theta}}$$

$$T_{av} = \int_0^{\infty} T(h) \alpha(h) \exp \left(-\int_0^h \alpha(h') dh' \right) dh / \int_0^{\infty} \alpha(h) \exp \left(-\int_0^h \alpha(h') dh' \right) dh$$

$$\tau(\lambda) = \tau_{O_2}(\lambda) \exp[-(h - h_c)/h_{O_2}] + \bar{\varphi}_{H_2O}(\lambda) Q + \psi_w(\lambda) W$$

$$h_{O_2} = 5300 \text{ m} \quad \tau_{O_2}(\lambda) = 0.045 \quad \bar{\varphi}_{H_2O}(\lambda) \approx 0.1076 \text{ cm}^2/\text{g} \quad \nu_2 \approx 94 \text{ GHz}$$

Катков В. Ю. Полуэмпирическая модель поглощения MM и СБММ радиоволн атмосферным водяным паром // Радиотехника и электроника. 1997. Т.42. № 12. С. 1441.

Two-wave measurements of integral moisture content -Q and cloud droplet fraction - W

$$\begin{aligned} \lambda_1 &= 13.5 \text{ mm} & \tau(\lambda_1) &= \tau_{O_2}(\lambda_1) + \varphi_{H_2O}(\lambda_1) \cdot Q + \psi_w(\lambda_1) \cdot W \\ \lambda_2 &= 8 \text{ mm} & \tau(\lambda_2) &= \tau_{O_2}(\lambda_2) + \varphi_{H_2O}(\lambda_2) \cdot K_1 \cdot Q + \psi_w(\lambda_2) \cdot W \end{aligned}$$

measurement of the optical thickness of the atmosphere in the transparency windows of 1 and 3 mm

$$\tau(\nu_\alpha), \alpha = 1, 2 \quad \tau(\nu_\alpha) = \tau_{O_2}(\nu_\alpha) + \varphi_{H_2O}(\nu_\alpha) \cdot Q + \psi_w(\nu_\alpha) \cdot W$$

$$\nu_1 \approx 90 - 110 \text{ GHz} \quad \nu_2 \approx 200 - 220 \text{ GHz} \quad \nu_3 \approx 56.7 \text{ GHz}$$

$$d(\theta) = k \cdot T_b(\theta) + A \quad d_0 = k \cdot T_0 + A$$

$$d_0; \quad d(\theta_0), d(\theta_1), d(\theta_2), d(\theta_3), \dots, d(\theta_{10})$$

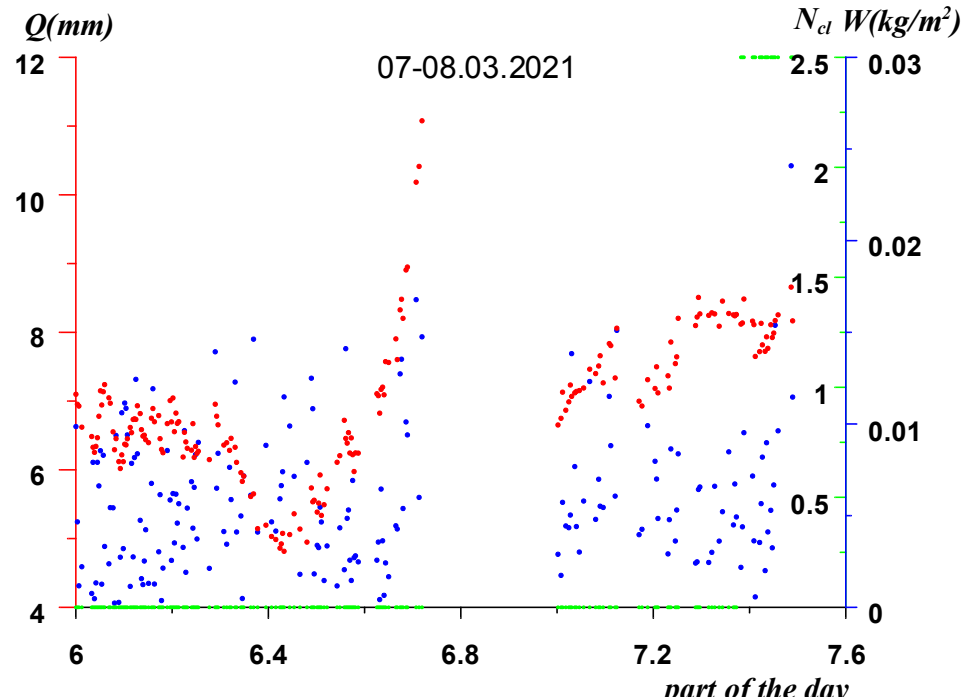
Atmospheric calibration

$$\ln(k[T_{av} - 2.73]) \quad d_0 = k \cdot T_0 + A$$

$$\ln(d_0 - d(\theta)) = -\frac{\tau}{\cos \theta} + \ln(k[T_{av} - 2.73])$$

$$T_{cp} = \frac{T_0 - 2.73 \cdot \left[e^{-\tau \sec \theta_2} \frac{n(d_0) - n(\theta_1)}{n(\theta_2) - n(\theta_1)} - e^{-\tau \sec \theta_1} \frac{n(d_0) - n(\theta_2)}{n(\theta_2) - n(\theta_1)} \right]}{1 - \left[e^{-\tau \sec \theta_2} \frac{n(d_0) - n(\theta_1)}{n(\theta_2) - n(\theta_1)} - e^{-\tau \sec \theta_1} \frac{n(d_0) - n(\theta_2)}{n(\theta_2) - n(\theta_1)} \right]}$$

$$\tau_0 = \tau_w + \tau \quad \tau_0 = \ln(k(T_{cp} - 2.73)) - \ln|d_0 - d(\theta=0)| - k(T_0 - (T_{cp} - 2.73))$$



Comparative analysis of tipping-curve methods

$$T_R(\theta) = T_{cp} \left(1 - e^{-\frac{\tau}{\cos \theta}} \right) + 2.73 \cdot e^{-\frac{\tau}{\cos \theta}}$$

$$d(\theta) = k \cdot T_R(\theta) + A \quad \theta_1 < \theta_2 < \theta_3$$

Метод 1

$$\tau = \frac{1}{\left(\frac{1}{\cos \theta_3} - \frac{1}{\cos \theta_2} \right)} \ln \left\{ \frac{d(\theta_2) - d(\theta_1)}{d(\theta_3) - d(\theta_2)} \cdot \frac{\exp \left[\tau \left(\frac{1}{\cos \theta_3} - \frac{1}{\cos \theta_2} \right) \right] - 1}{\exp \left[\tau \left(\frac{1}{\cos \theta_2} - \frac{1}{\cos \theta_1} \right) \right] - 1} \right\}$$

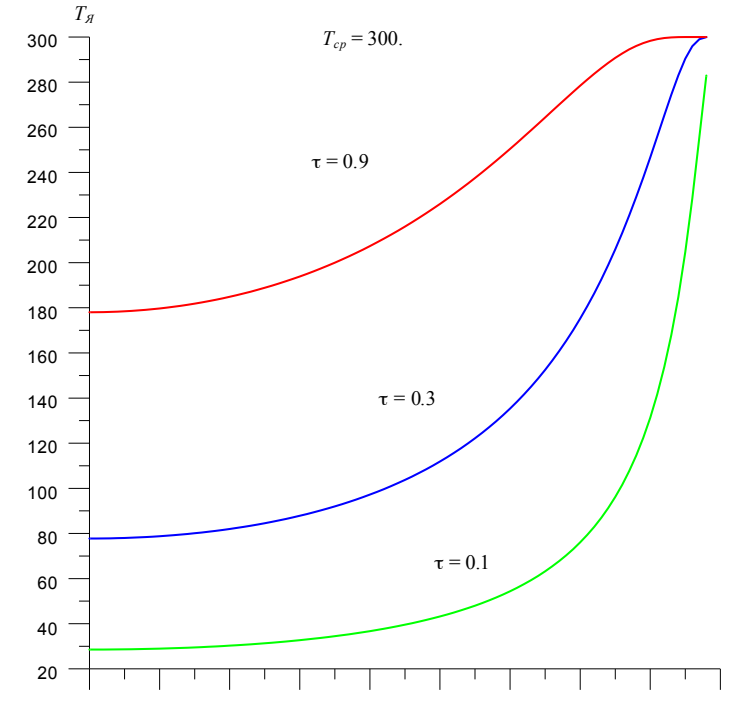
И.Т. Бубукин, К.С. Станкевич Радиометрия температурной плёнки морской поверхности // Успехи современной радиоэлектроники.- 2006.- №11.- С.39-55.

Метод 2 $\tau = \frac{1}{\left(\frac{1}{\cos \theta_2} - \frac{1}{\cos \theta_1} \right)} \ln \left(\frac{d_0 - d(\theta_1)}{d_0 - d(\theta_2)} \right) + \Delta$

$$d_0 = d(\theta_3), \quad \Delta = \frac{1}{\left(\frac{1}{\cos \theta_2} - \frac{1}{\cos \theta_1} \right)} \ln \left(\frac{1 + b \cdot h_w \cdot s \left(\frac{\tau}{\cos \theta_1} \right) / T_0}{1 + b \cdot h_w \cdot s \left(\frac{\tau}{\cos \theta_2} \right) / T_0} \right)$$

$$s(y) = \sum_{k=1}^{\infty} \frac{y^k}{(k \cdot k!)} \quad b - \text{градиент температуры в атмосфере} \\ h_w - \text{толщина водяных паров в атмосфере}$$

$$Y(\tau) = \frac{d(\theta_2) - d(\theta_1)}{d(\theta_3) - d(\theta_2)} = \frac{T_R(\theta_2) - T_R(\theta_1)}{T_R(\theta_3) - T_R(\theta_2)} = \frac{\exp \left(-\frac{\tau}{\cos \theta_2} \right) - \exp \left(-\frac{\tau}{\cos \theta_1} \right)}{\exp \left(-\frac{\tau}{\cos \theta_3} \right) - \exp \left(-\frac{\tau}{\cos \theta_2} \right)}$$

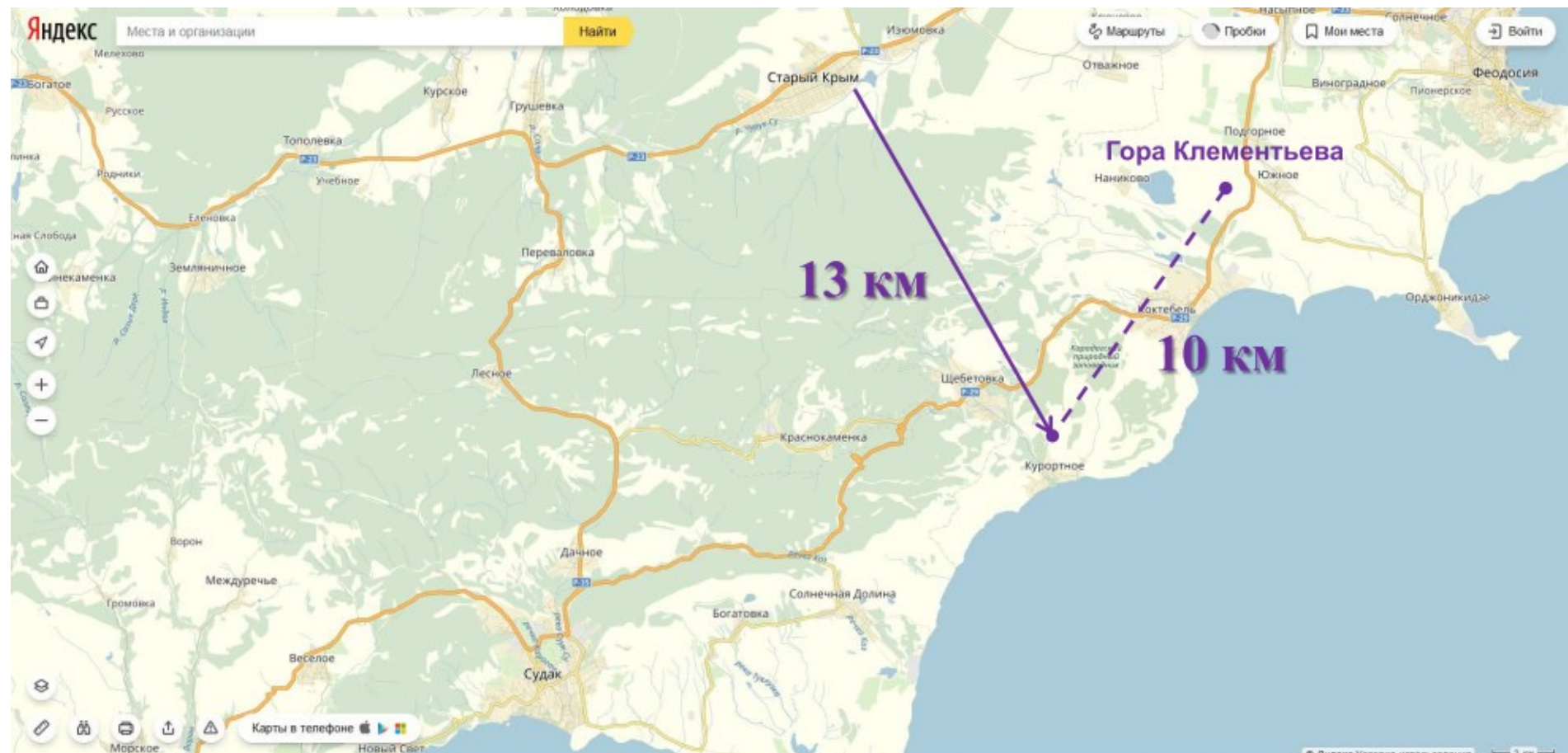


Dependence of the brightness temperature of the atmosphere on the zenith angle for 1, 3 and 8 mm

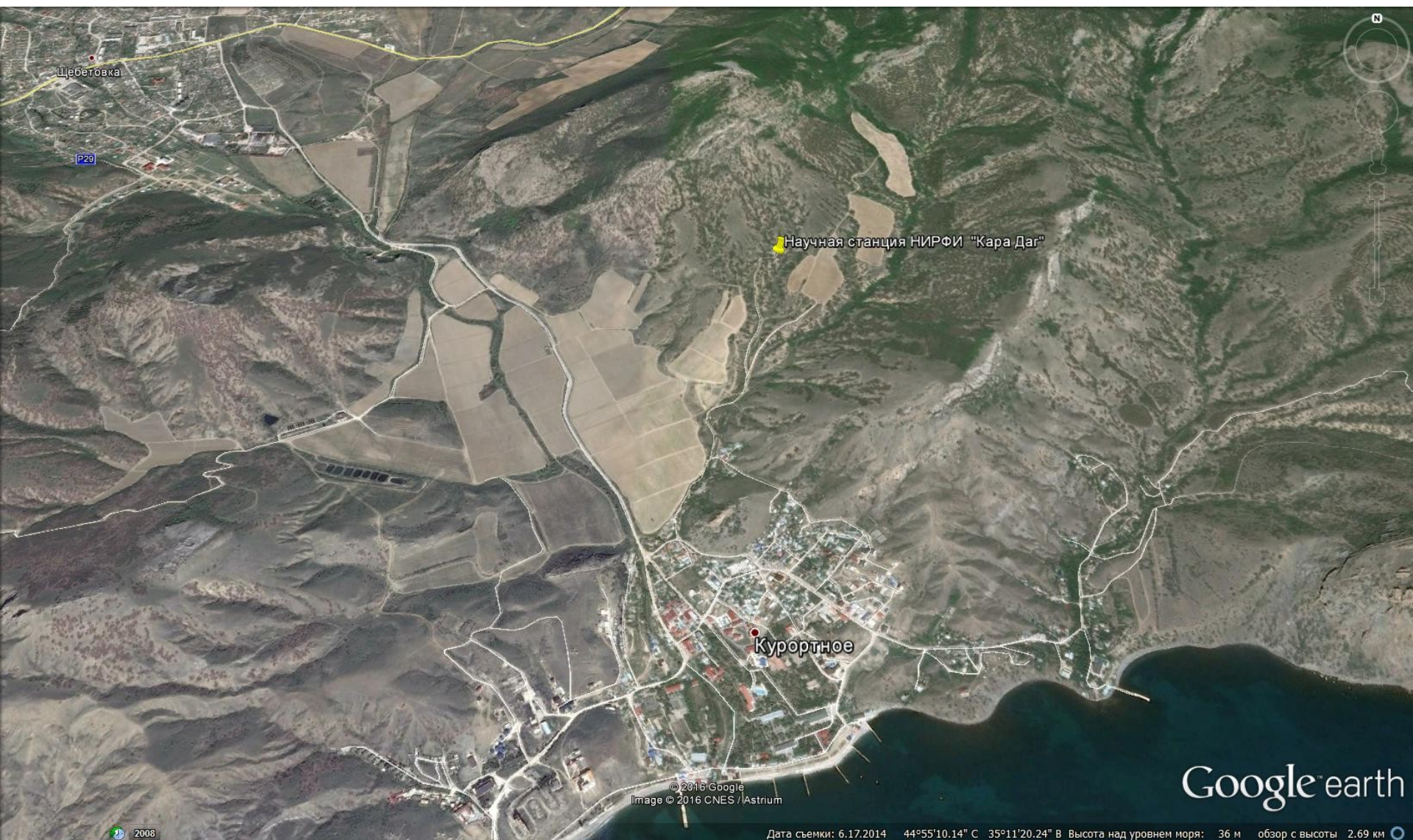
Кисляков А.Г., Станкевич К.С. Исследование тропосферного поглощения радиоволн радиоастрономическими методами // Известия высших учебных заведений. Радиофизика. 1967. Т. 10. № 9-10. С. 1244-1265

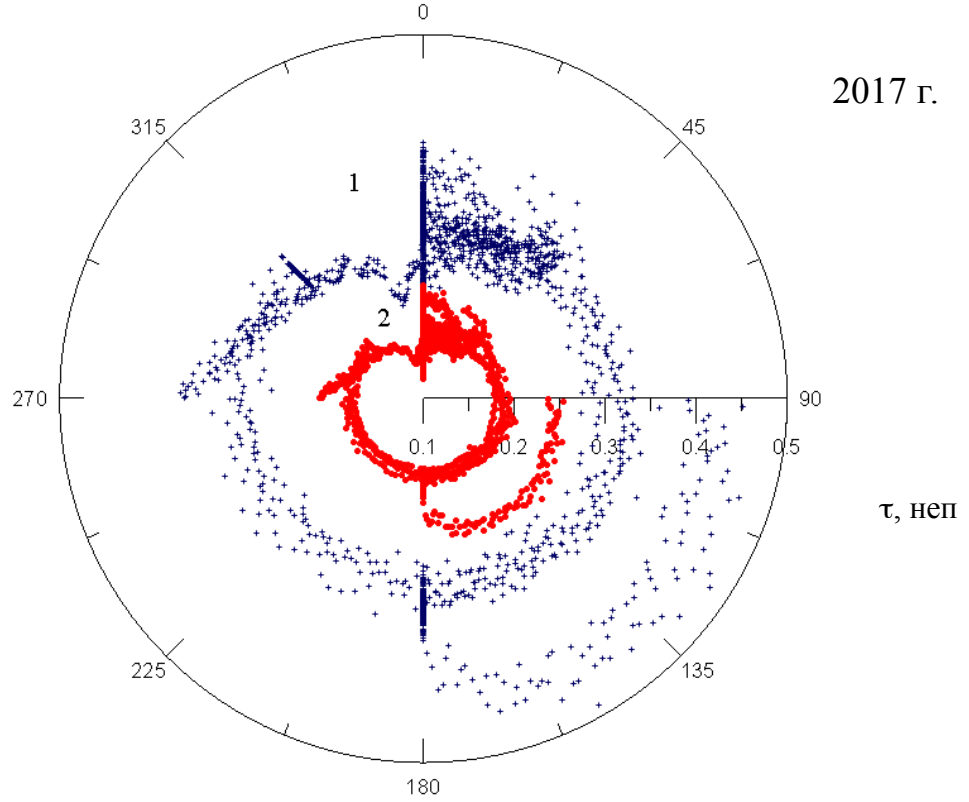
Степаненко В.Д., Щукин Г.Г., Бобылев Л.П., Матросов С.Ю. Радиотеплолокация в метеорологии. Л.: Гидрометеоиздат, 1987.

Choosing the location of an optical telescope before the war



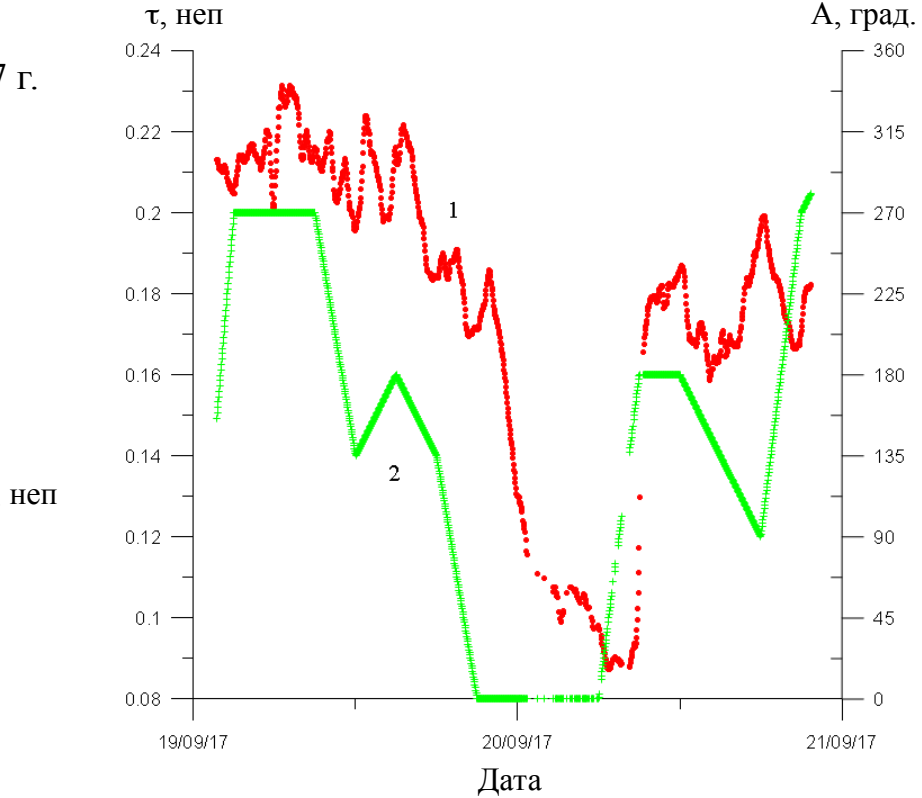
**The results of measurements of atmospheric transparency parameters
and their relationship to climatic features at the location of the Karadag sites.**





2017 г.

τ , неп

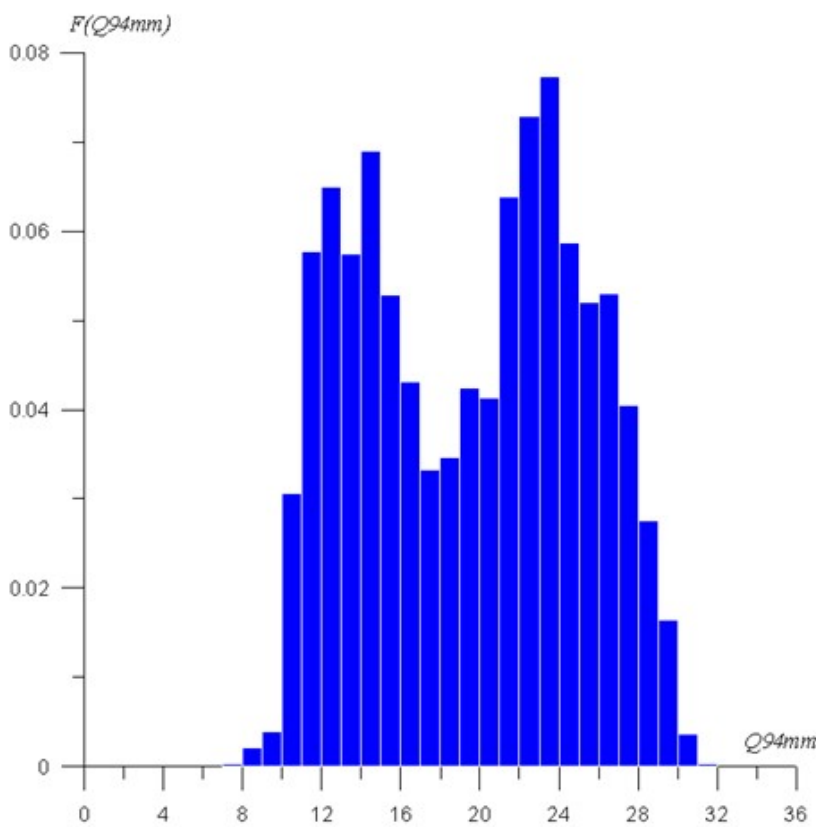


Дата

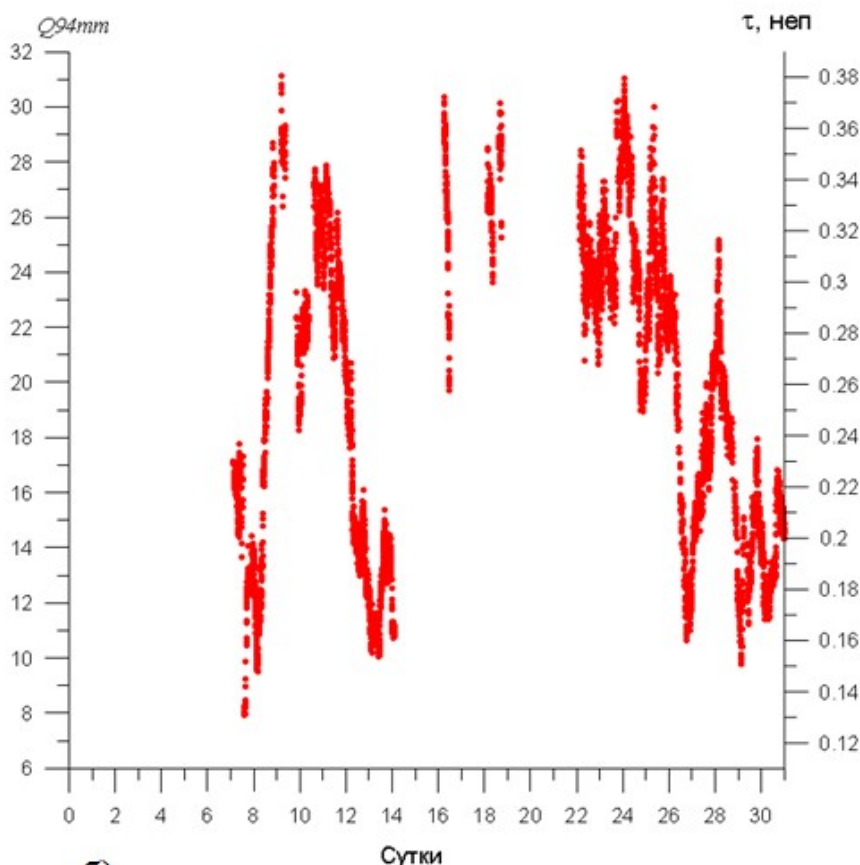
A graph of the azimuthal dependence of atmospheric absorption in radiometric channels of 3 mm (red, dots - 2) and 2 mm (blue, crosses - 1). Atmospheric absorption is postponed along the radial axis, and the azimuthal axis shows the direction from which the wind blows A (deg.) in the measurement area from July 29 to August 2, 2017. Zero degrees corresponds to the north direction.

Atmospheric absorption measurement graphs for a wavelength of 3 mm (red, dots - 1) are the left scale and the direction from which the wind blows A (green, crosses - 2) are the right scale from September 19 to 21, 2017 at the Karadag sites. Zero degrees corresponds to the north direction. During a time interval of about 8 hours, there is a sharp decrease in absorption for a wavelength of 3 mm. When the wind direction changes to the north, absorption decreases with a certain time delay.

2019 г.

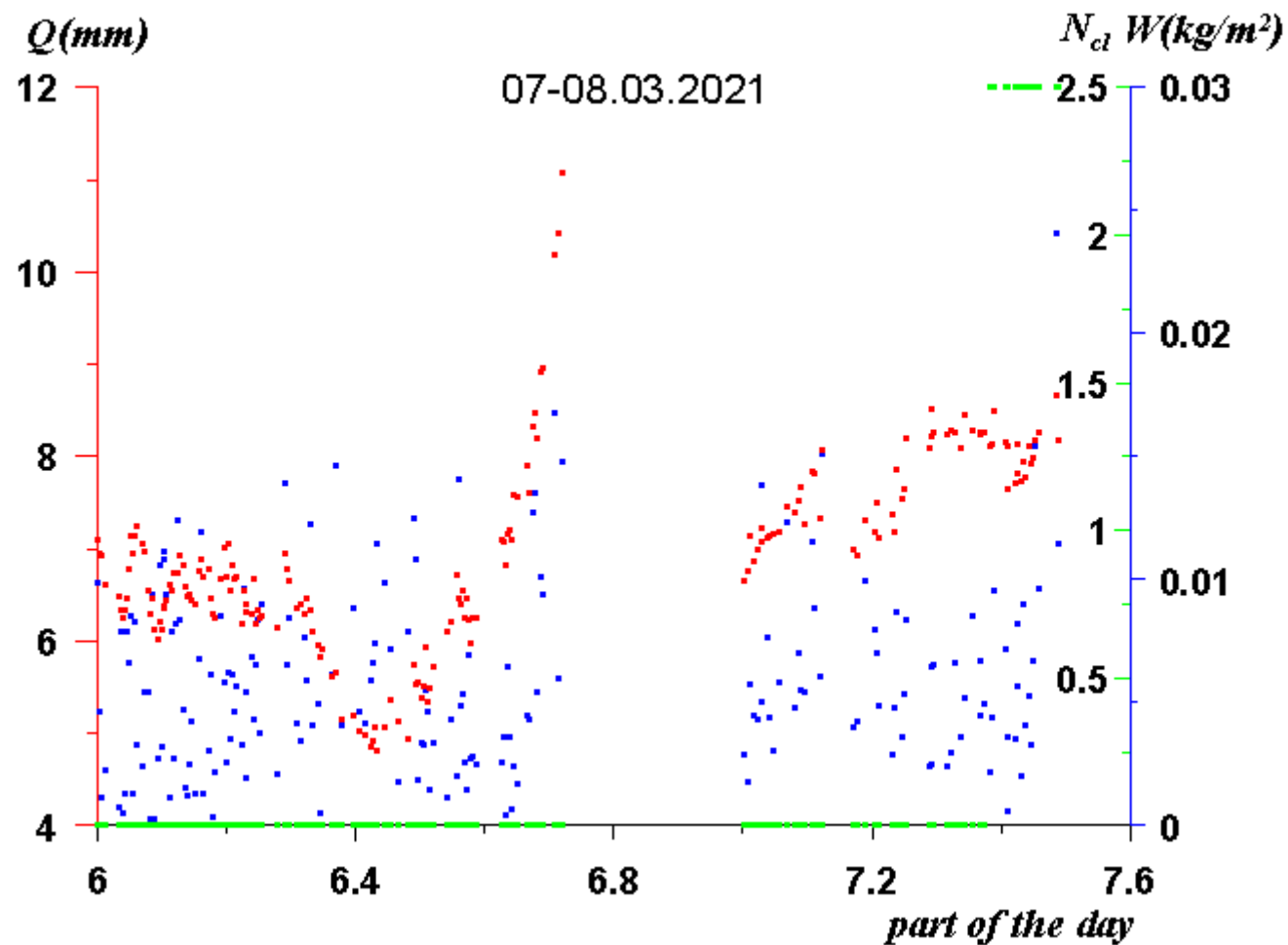


a)

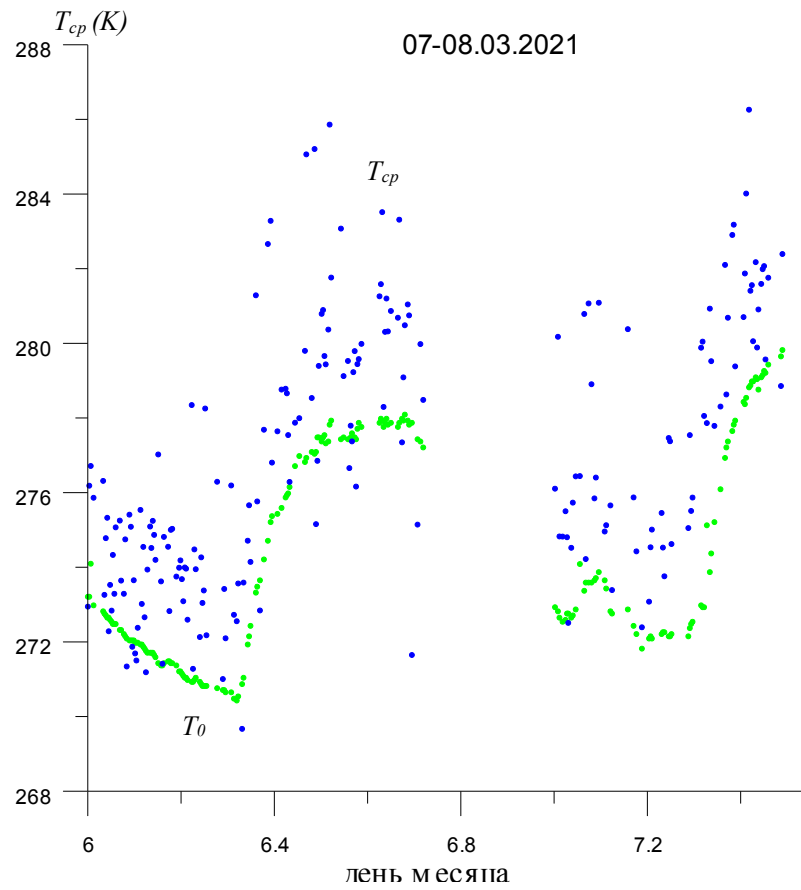


б)

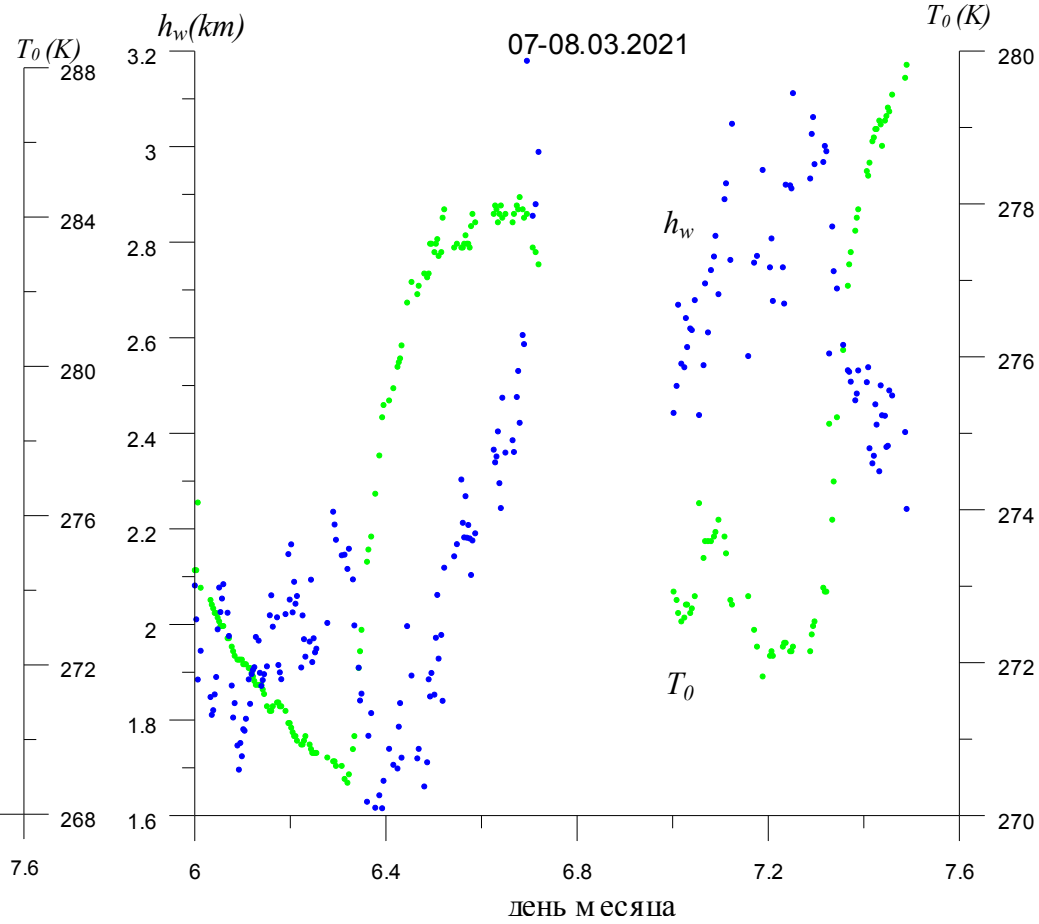
- a) A histogram of the measured values of the integral moisture content in the atmosphere in millimeters of deposited moisture for a wavelength of 3 mm at the Karadag sites with two maxima for August 2019. The histogram is based on 5,655 measurements; b) the time dependence (horizontal axis in fractions of a day from the beginning of the month) of the values of the integral moisture content in the atmosphere in millimeters of deposited moisture on the Karadag sites in August 2019



Atmospheric moisture content is Q (mm) (red dots, left scale), cloud water storage is W (kg/m^2) (blue dots, right scale) measured at a wavelength of 3 mm and the proportion of the sky covered with clouds according to meteorological data is N_{cl} (green, medium scale) Karadag, 07-08.03.2021.

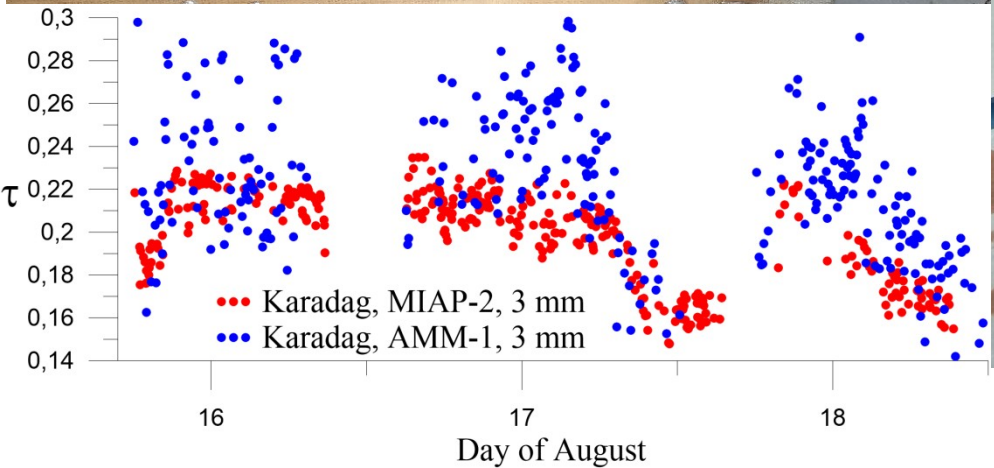
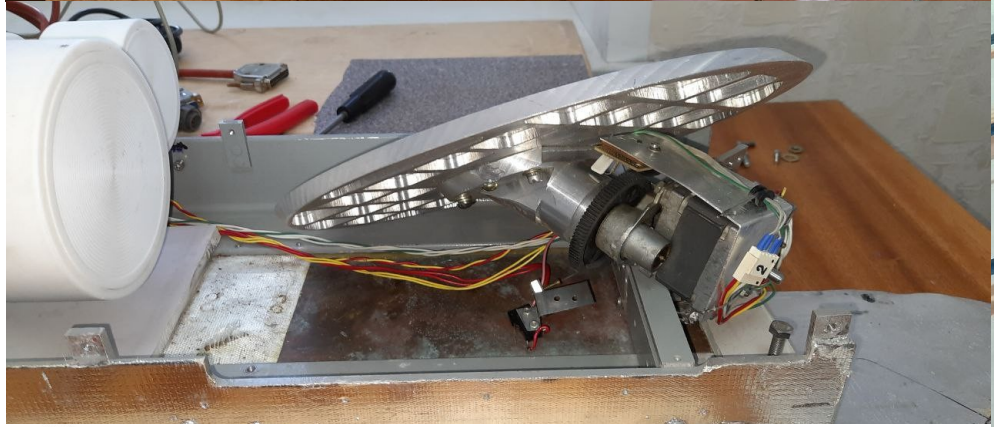


Surface (green dots) and average temperature (blue dots) of the atmosphere measured at a wavelength of 3 mm Karadag, 07-08.03.2021

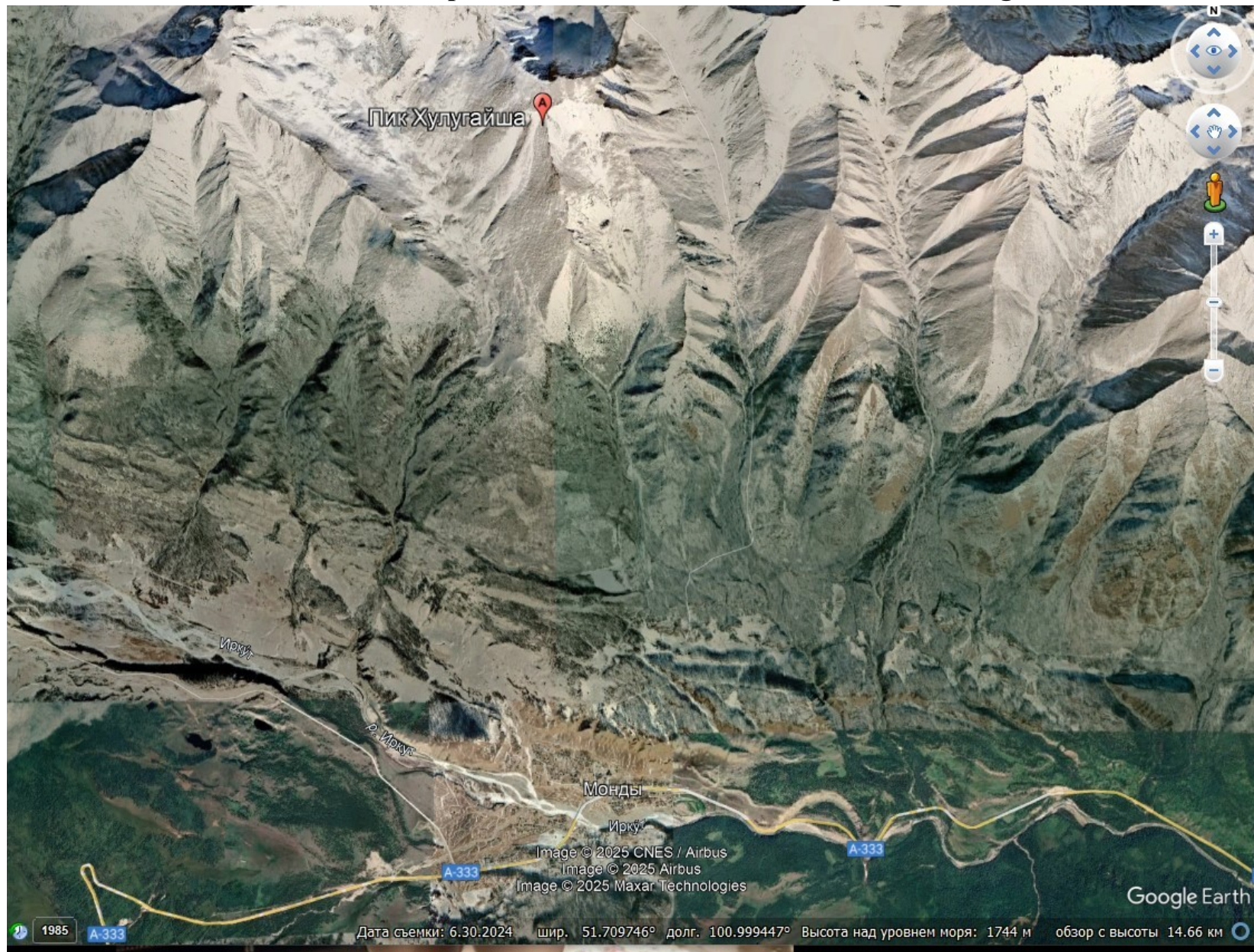


The thickness of the water vapor layer (blue dots) and the surface temperature (green dots) of the atmosphere as measured at a wavelength of 3 mm Karadag, 07-08.03.2021

Ремонт и калибровка МИАП-2



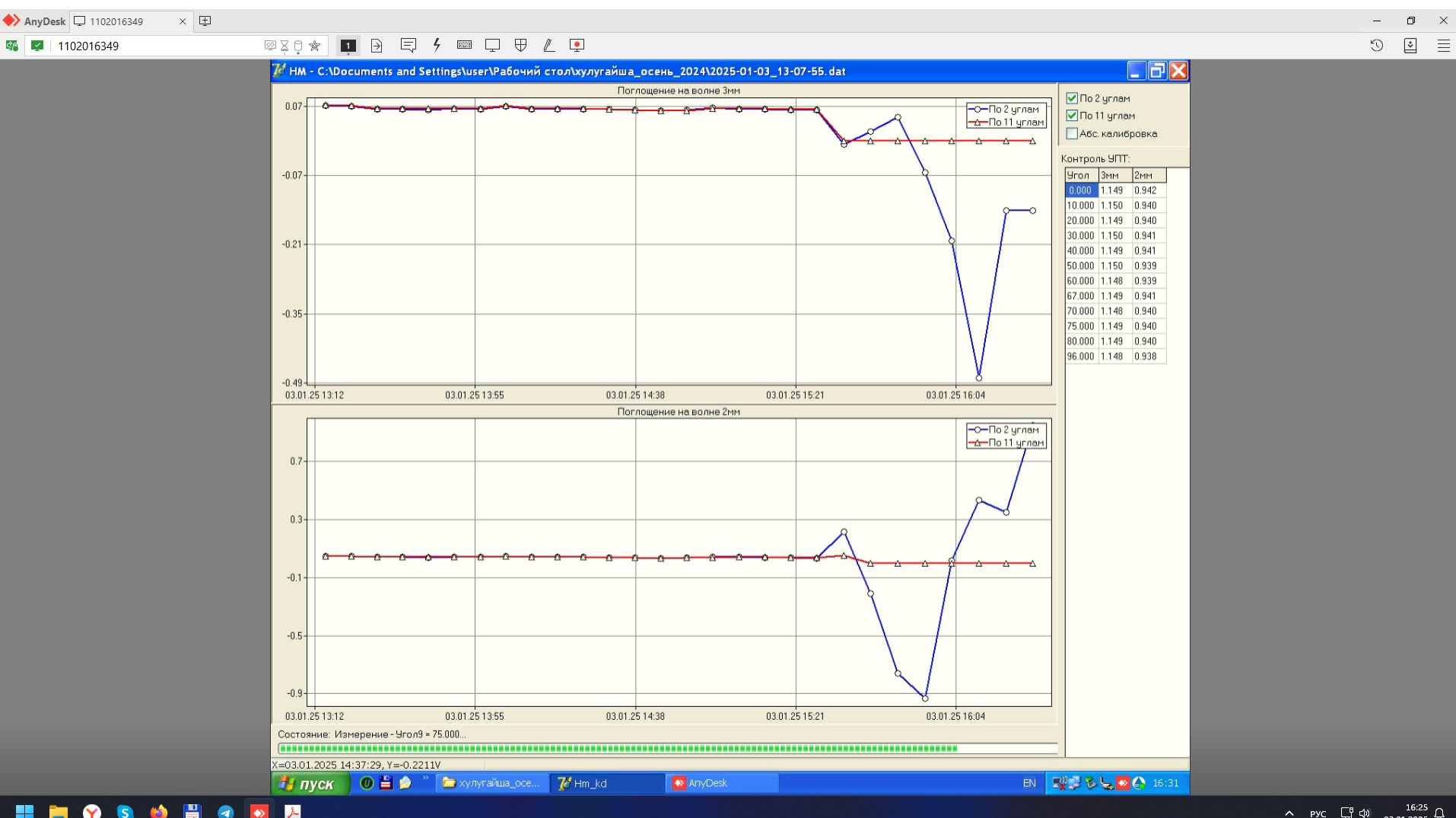
**The results of measurements of atmospheric transparency parameters
and their relationship to the climatic features of the peak " Khulugaisha ".**



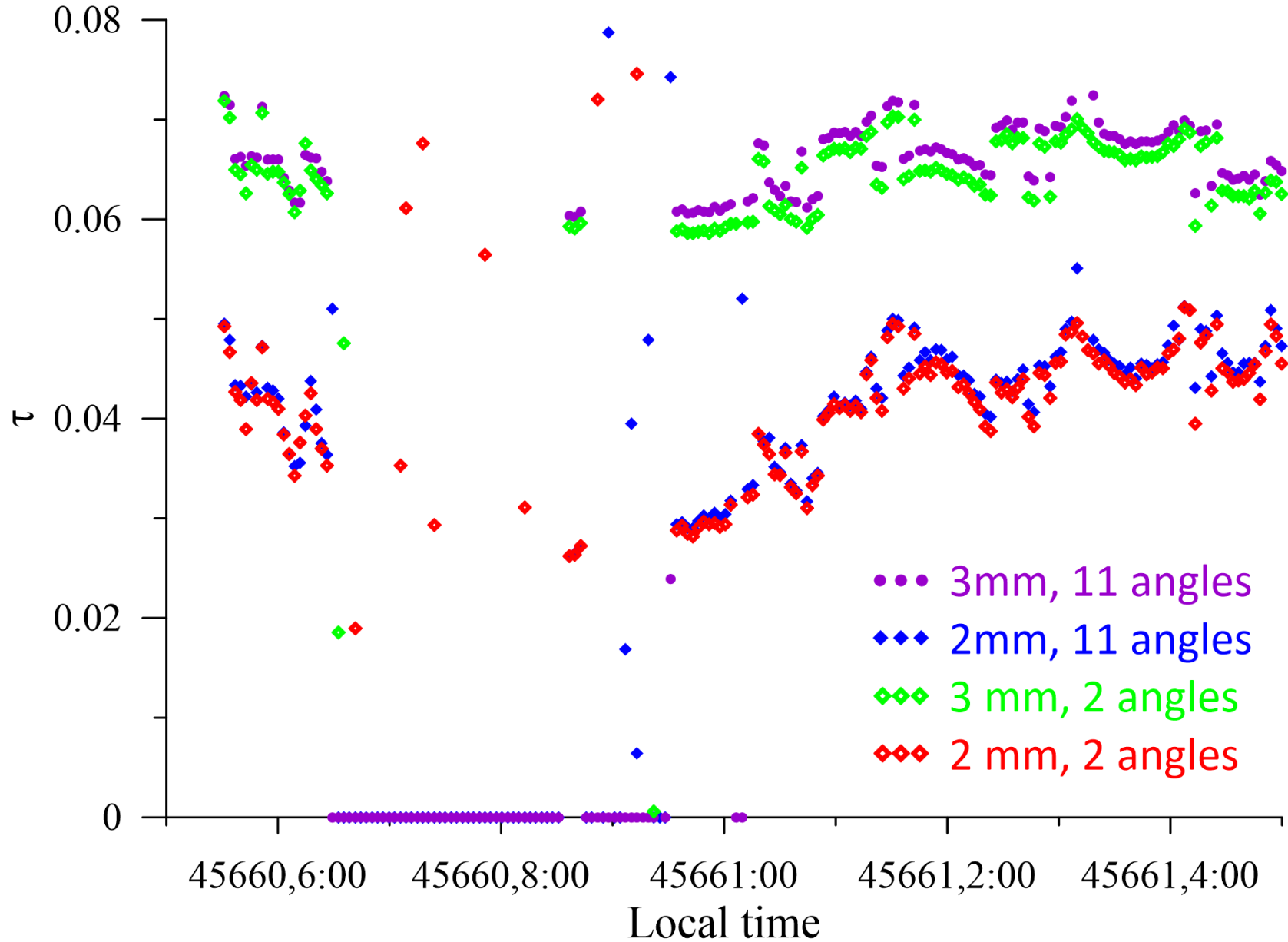
Хулугайша Khulugaisha высота 2794 м

метеостанция Монды Monds 8 км на юг, (Монды 51° 41' с.ш., 100° 59' в.д.; 1259 м)

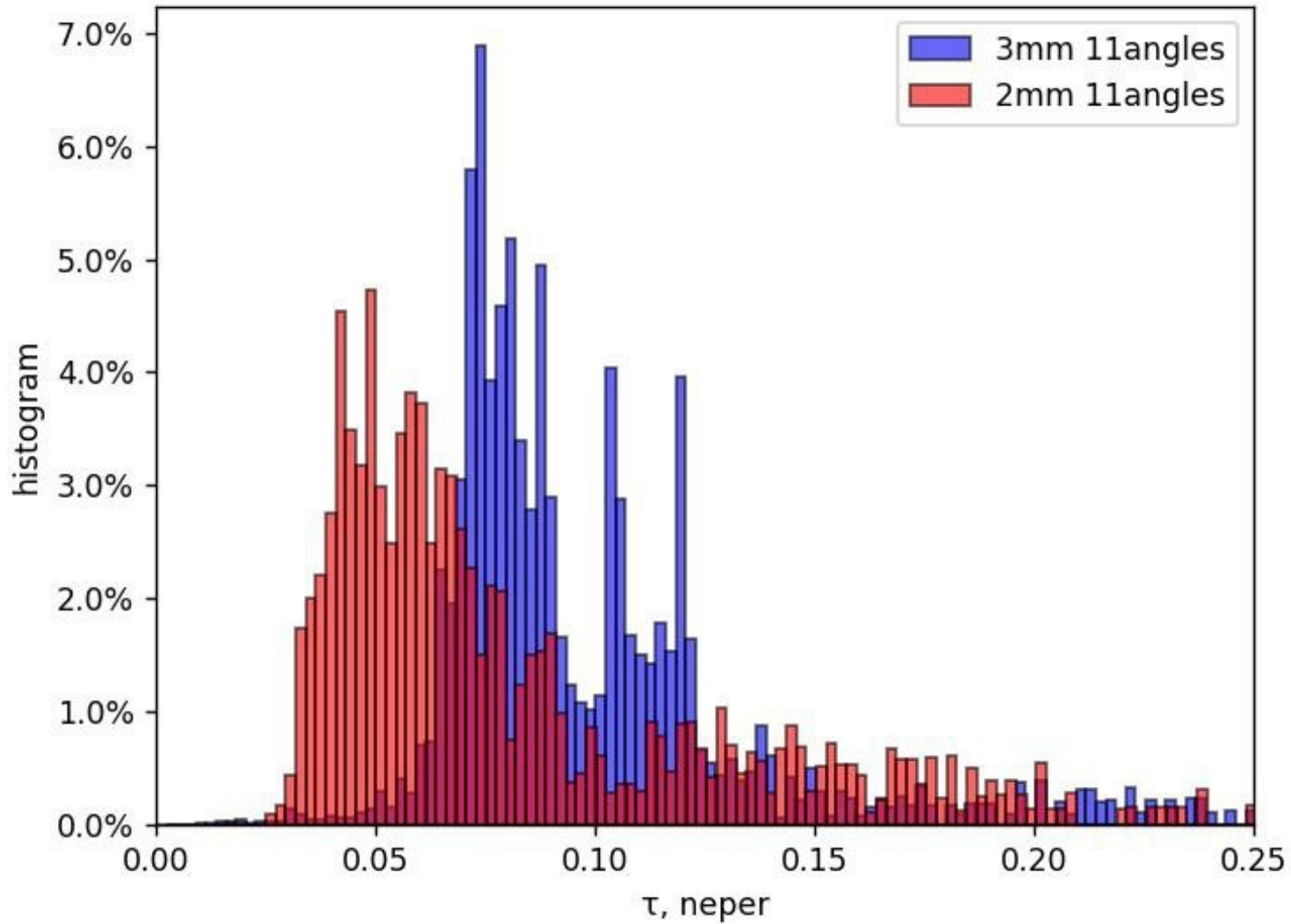




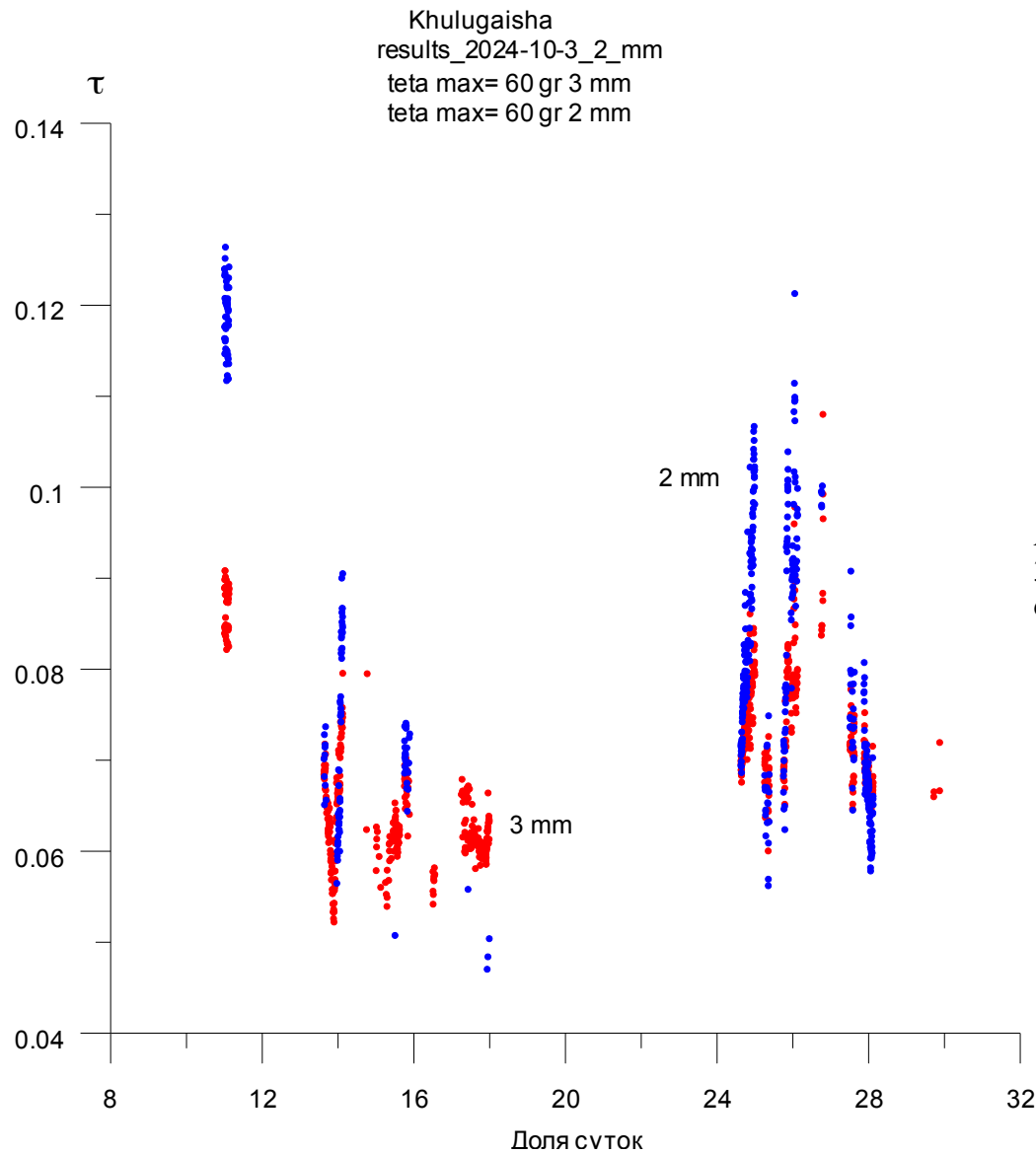
При малых поглощениях метод **11 углов** работает лучше, чем метод **2 углов**.



При совсем малых поглощениях чувствительности приемников МИАП не хватает, либо приемники работают некорректно при низких температурах.

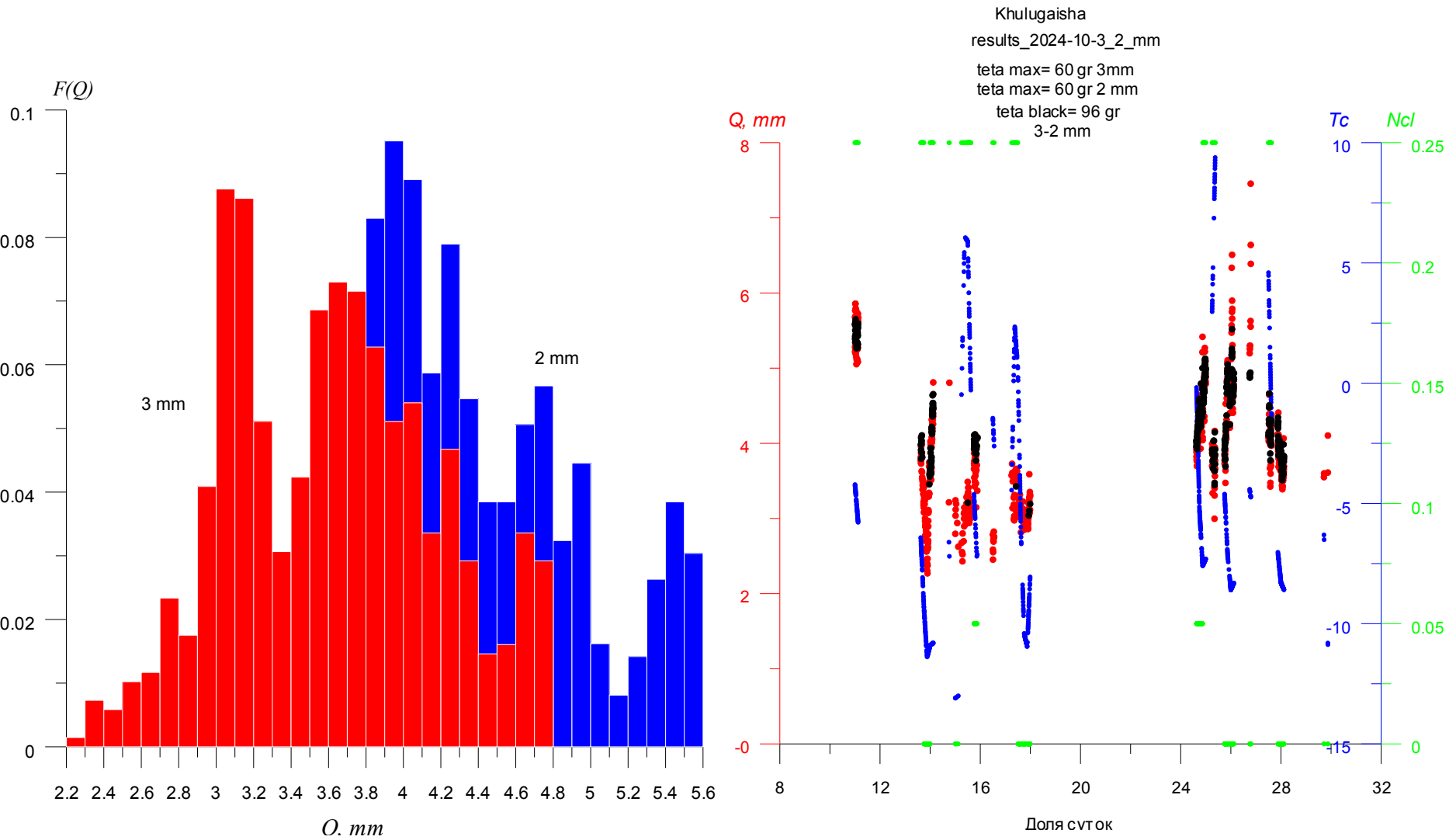


Данные с 12.03.2025 по 28.03.2025, гистограммы на графике соответствуют 95,1 % и 98,7 % от полного времени измерений.
Значительную часть времени наблюдается инверсия, поглощение на 2мм меньше, чем на 3мм. При ухудшении погоды (правые максимумы) поглощение на 3мм < 2мм.



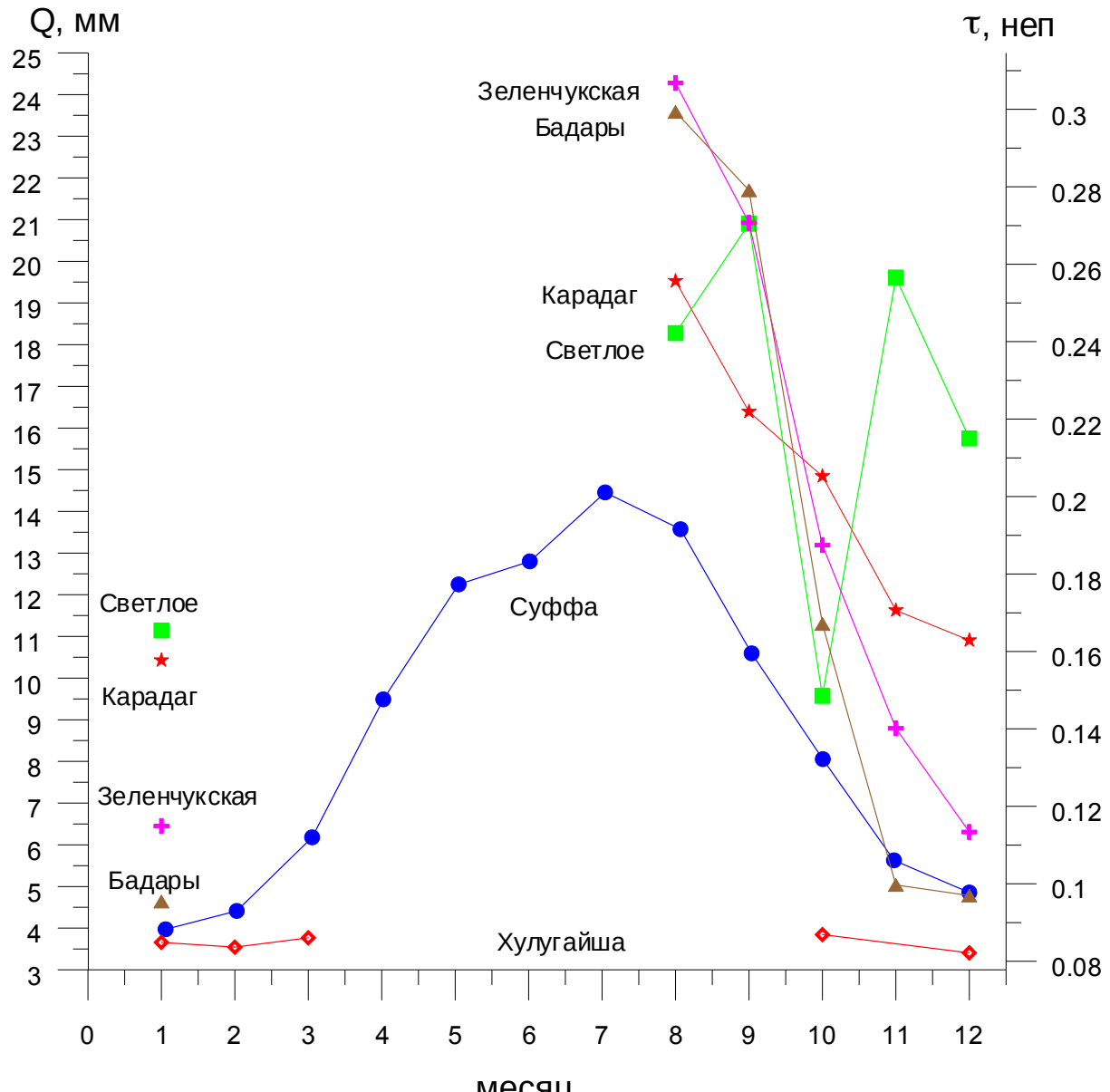
Atmospheric absorption measured at a wavelength of
 3 mm (red dots) and at a wavelength of 2 mm (blue
 dots) Khulugaisha, October 2024

$$\tau(\lambda) = \tau_{O_2}(\lambda) \cdot \exp[-(h - h_c)/h_{O_2}] + \bar{\varphi}_{H_2O}(\lambda)Q + \psi_w(\lambda)W$$



Histogram of atmospheric moisture content measured at a wavelength of 3 mm (red) and at a wavelength of 2 mm (blue) Khulugaisha, October 2024

Atmospheric moisture content is Q (mm) measured at a wavelength of 3 mm (red dots, left scale) and at a wavelength of 2 mm (black dots, left scale), surface temperature is $T(C)$ (blue dots, middle scale) and the proportion of the sky covered with clouds according to meteorological data is Ncl (green, right scale) Khulugaisha, October 2024.



Graphs of measurements of integral moisture content with clouds of less than 2.5 points (left scale) for 1981-1991. for "Suffa" – blue dots, for other sites from August 2019 to January 2020: "Karadag" – red stars, "Svetloye" – green squares, "Zelenchukskaya" – purple crosses, "Badary" – brown triangles, "Khulugaisha" – red diamonds.

**Спасибо за
внимание!**

Работа поддержана грантом РНФ № 25-79-20019